Liquid Metal Reconfigurable Patch Antenna for Linear, RH, and LH Circular Polarization With Frequency Tuning

Reconfiguration d'une antenne patch par métal liquide pour une polarisation linéaire, circulaire RH et LH avec réglage de fréquence

Arcesio Arbelaez, Ian Goode, Juan Gomez-Cruz, Carlos Escobedo, and Carlos E. Saavedra

***Abstract*— A microstrip circular patch antenna with frequency and polarization reconfigurability using liquid metal is presented. The antenna has a C-shaped slot cut at the center of the patch and reconfigurability is achieved using two putty containers and liquid metal to switch between four different states. Linear polarization (LP) is observed at 5.83 GHz when there is no liquid metal inside the containers. Depositing two liquid metal droplets in the containers yields circular polarization (CP) at 6 GHz. The right-hand CP (RHCP) is obtained when the right-most container is filled, and the left-hand CP (LHCP) is obtained when the leftmost container is filled with the liquid metal. When all containers are filled, LP is observed at 6.15 GHz. For the LP case, the antenna has a measured gain of 2.68 dB when all containers are filled and a measured gain of 3 dB when the containers are empty, and the axial ratios (ARs) are 19.65 dB (filled containers) and 23.74 dB (empty containers). When the LHCP is activated, the gain is 2.44 dB and the AR is 0.54 dB at 6 GHz. For RHCP, the gain is 2.37 dB and the AR is 1.5 dB at 6 GHz.**

***Résumé*— Une antenne patch circulaire à ligne microruban avec une reconfiguration de la fréquence et de la polarisation par l'utilisation d'un métal liquide est présentée. L'antenne a une fente en forme de C découpée au centre du patch et la reconfiguration est obtenue en utilisant deux conteneurs et du métal liquide qui bascule entre quatre états différents. Une polarisation linéaire (LP) est observée à 5,83 GHz lorsqu'il n'y a pas de métal liquide à l'intérieur des conteneurs. Le dépôt de deux gouttelettes de métal liquide dans les conteneurs produit une polarisation circulaire (CP) à 6 GHz. La CP à droite (RHCP) est obtenue lorsque le conteneur le plus à droite est rempli, alors que la CP à gauche (LHCP) est obtenue lorsque le conteneur le plus à gauche est rempli de métal liquide. Lorsque tous les conteneurs sont remplis, la LP est observée à 6,15 GHz. Pour le cas LP, l'antenne a un gain mesuré de 2,68 dB quand l'ensemble des conteneurs sont remplis et un gain mesuré de 3 dB lorsqu'ils sont vides et les ratios axiaux (ARs) sont de 19,65 dB (conteneurs remplis) et 23,74 dB (conteneurs vides). Lorsque la LHCP est activée, le gain est de 2,44 dB et l'AR est de 0,54 dB à 6 GHz. Alors que pour RHCP active, le gain est de 2,37 dB et l'AR est de 1,5 dB à 6 GHz.**

***Index Terms*— Circular patch, circular polarization (CP), fluidic, linear polarization (LP), liquid metal, microstrip antenna, reconfigurable, tunable.**

I. Introduction

When some aspect of an antenna's functionality is adjustable, the antenna is said to be reconfigurable. Although frequency tuning is one of the most commonly studied forms of antenna reconfigurability, techniques for adjusting antenna radiation patterns, their directivity or their polarization have also garnered much interest [1]–[5].

Antenna reconfigurability is often accomplished using semiconductor devices, such as varactors, diodes, or transistors, all of which can introduce distortion on the transmit path or deteriorate noise figure on the receive path of a wireless link [6]. Microelectromechanical systems (MEMS) have also been used to reconfigure antennas and while they do not compromise the system noise or linearity performance, MEMS typically require high operating voltages and their mean-time-to-failure (MTTF) is lower than that of a semiconductor device. Diodes are commonly used, but they introduce distortion at high RF power levels. In [7], the effects of the p-i-n diode on the antenna performance are shown by using a lumped model,

Manuscript received October 25, 2018; revised January 29, 2019; accepted March 2, 2019. Date of current version August 21, 2020. This work was supported by the Natural Sciences and Engineering Research Council (NSERC) under Grant RGPIN-2016-04784. *(Corresponding author: Arcesio Arbelaez.)*

A. Arbelaez, I. Goode, and C. E. Saavedra are with the Department of Electrical and Computer Engineering, Queen's University, Kingston, ON K7L 3N6, Canada (e-mail: arcesioarbelaez@gmail.com; ian.goode@queensu.ca; saavedra@queensu.ca).

J. Gomez-Cruz and C. Escobedo are with the Department of Chemical Engineering, Queen's University, Kingston, ON K7L 3N6, Canada (e-mail: 17jmgc@queensu.ca; ce32@queensu.ca).

Associate Editor managing this paper's review: Aldo Petosa.

Digital Object Identifier 10.1109/CJECE.2019.2904898

and the efficiency gets lower when the frequency is increased due to the loss of the diode; the frequency is modified by the switch capacitance and the diode's OFF-resistance decrease the gain of the antenna. The use of fluids to tune the response of antennas and microwave components holds significant promise on account of their high power handling capability, longer lifespan compared to MEMS devices, and low-noise characteristics [8]–[11]. A desired characteristic of using liquid metal is the linear behavior of the structure, this is because no semiconductor devices are involved in the switching process between states [10]. In addition, liquid metal-based reconfigurable devices can support high power in comparison with conventional methods [12].

Patch antennas have been commonly used to get polarization reconfigurability by cutting U-shaped slots in the copper trace of the antenna to alter their current distributions [13], [14]. Other designs have shown the possibility to get frequency diversity and switchable polarization based on the multiband antennas and diodes [15] or linear polarization (LP) diversity using the patch antennas and diodes to modify the behavior of the antenna [16].

In this paper, a low complexity antenna with reconfigurable frequency (four states) and polarization (three states) is proposed by using only two liquid metal switches. LP and circular polarizations (CPs) (right-hand/left-hand) are achieved using only two putty containers and the liquid metal Eutectic Gallium-Indium (EGaIn) to get four states by shorting the surface of a microstrip circular patch across a C-shaped slot in the copper trace of the antenna.

II. Reconfigurable Antenna Design

The circular patch antenna is depicted in Fig. 1. It is fed on the topside by a transmission line and matching network, and its backplane is fully grounded. The antenna was designed using a substrate with $\epsilon_r = 3.55$, $\tan\delta = 0.0027$, and a thickness of $h = 1.52$ mm (Rogers 4003C). The antenna was designed to radiate at a nominal frequency of 6 GHz and its radius, a, was calculated using [17]

$$a = \frac{F}{\left[1 + \frac{2h}{\pi F \epsilon_r}(ln(\pi F/2h) + 1.7726)\right]^{1/2}} \quad (1)$$

$$F = \frac{8.791 \times 10^9}{f_r\sqrt{\epsilon_r}} \quad (2)$$

where $f_r = 6$ GHz, v_c is the speed of the light in free space, ϵ_r is the relative permittivity of the substrate, and h is the height of the substrate. A C-shaped slot is milled out of the patch to generate CP by using two liquid metal switches. The table in Fig. 1 lists the antenna's dimensions. Note that the parameter g is the distance between the center of the circle and the bottom of the C-shaped slot.

An insulating film of polydimethylsiloxane (PDMS) protects the surface of the antenna except for two openings on the left and right arms of the C slot where the copper is exposed to the liquid metal. The gray rectangles shown in Fig. 2(a) represent the locations where liquid metal is deposited. The liquid metal drops were modeled as rectangular cuboids with a footprint of 1.3 mm × 1.1 mm. A more accurate geometrical model for the drops would be a semihemisphere but considering the small dimensions of the structure relative to wavelength, the cuboid shape is a good approximation. There is an overlap of 0.1 mm between the liquid metal and the copper metals on both sides of the slot to ensure a good electrical contact.

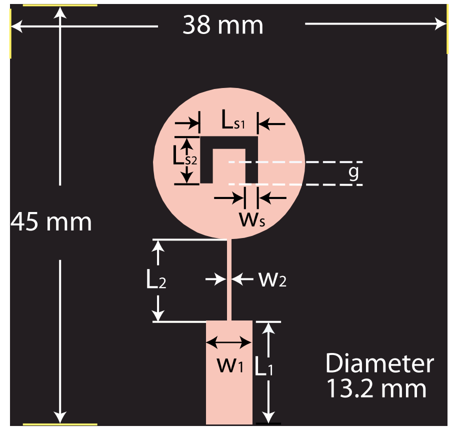

var.	W_1/L_1	W_2/L_2	L_{s1}	L_{s2}	W_s	g
(mm)	4/12	0.4/7.1	5	4.1	1.1	1.86

Fig. 1. Circular patch antenna with C-shaped slot.

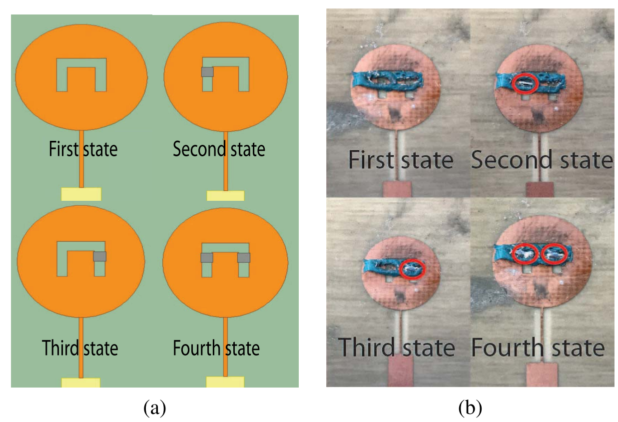

Fig. 2. Four antenna states. (a) First state LP at 5.83 GHz, second state LHCP at 6 GHz, third state RHCP at 6 GHz, and fourth state LP at 6.15 GHz. (b) Fabricated antenna.

The liquid metal drops are held in place at the two locations in the C slot using miniature containers made of putty. Liquid metal switches have some advantages previously mentioned. In addition, in the case of antennas, the loss due to the liquid metal drop is low because it is not switching the full flow of the antenna's current. The uniform distribution of the liquid metal on the top of the dielectric is also an advantage because, unlike a diode or a MEMS switch, there is no air gap between the conductor and the dielectric, and it might be connected to the antenna's cooper by using an fixed container. The liquid metal can be easily integrated to the planar antenna's technology.

In total, the antenna has four possible operating states as depicted in Fig. 2(a). The first state yields LP, which is the case when there is no liquid metal inside the containers as

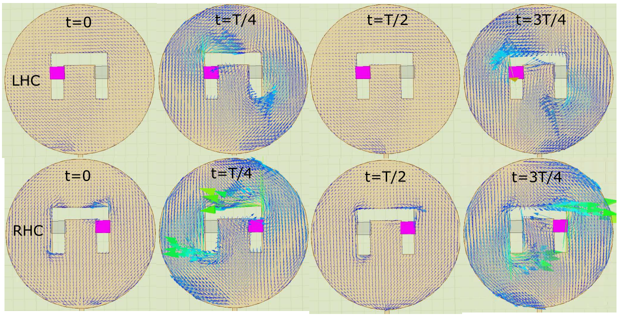

Fig. 3. Current distribution of the antenna, LHCP (top), and RHCP polarization (bottom).

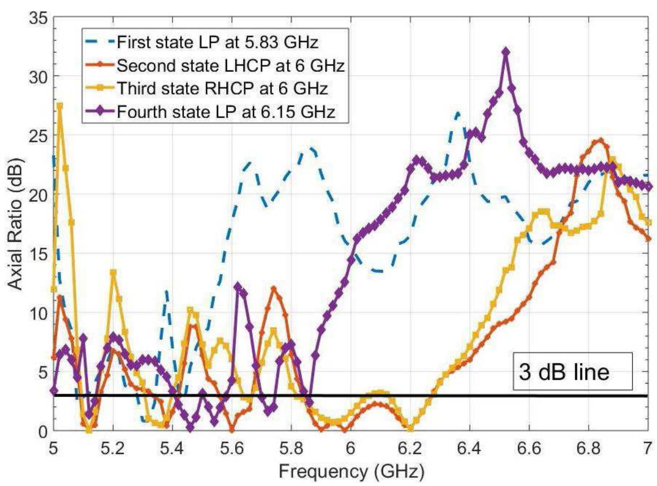

Fig. 4. Measured AR of the antenna for each of the four states.

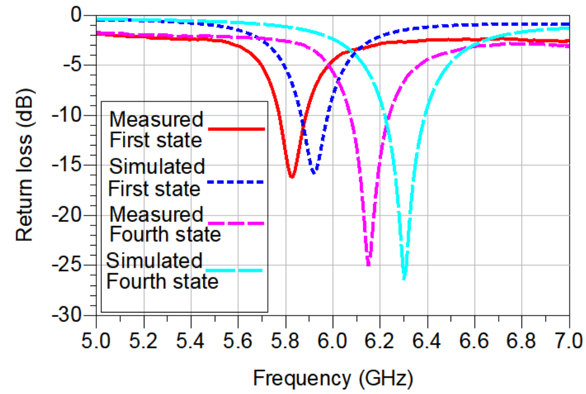

Fig. 5. Measured return loss first and fourth states LP.

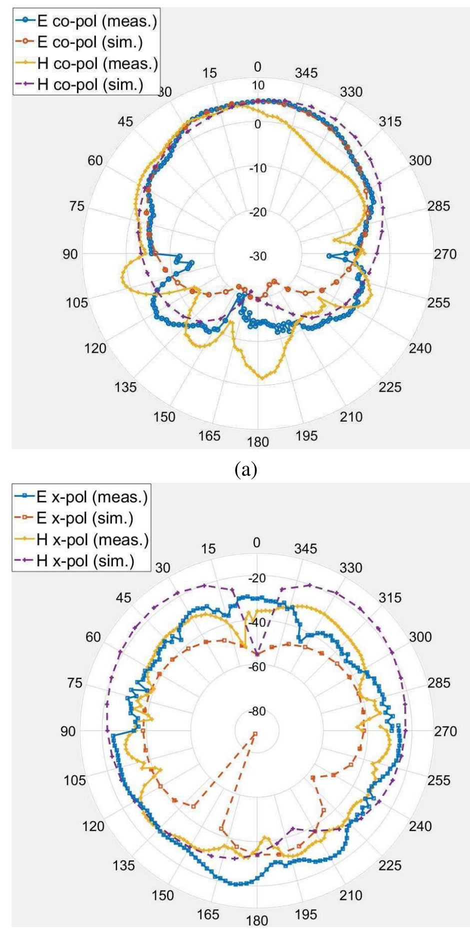

(a)

(b)

Fig. 6. Measured (a) co-pol and (b) x-pol radiation patterns in decibel for the first state (LP) at 5.83 GHz.

observed in Fig. 2(a). The second state is activated when the liquid metal is deposited into the left-side container. There is a short circuit connecting both sides of the slot, which excites two orthogonal degenerated modes with a 90° phase difference generating a clockwise rotation of the electric field or left-hand polarization. The third state is activated when the liquid metal is moved to the right side container, in this case, there is a right-hand polarization. A fourth state is obtained when the liquid metal is connecting both slots, which generates LP and a higher operating frequency due to the excitation of two orthogonal modes with no phase difference. A photograph of the fabricated antenna in the four different states is shown in Fig. 2(b). Fig. 3 shows the simulated electric surface current distribution during one-time cycle for both cases of CP.

The high efficiency of the antenna is maintained in all the states because the area of the liquid metal rectangles is small compared to the total surface of the antenna; the current distribution along the surface is modified but the current concentration around the liquid metal is small. A similar effect occurs for the antenna gain. The putty containers have a small area compared to the total surface of the antenna, for this reason, the gain of the antenna is not highly impacted.

III. Experimental Results

The antenna was fabricated on a Rogers 4003C substrate with 0.5-oz copper cladding using an LPKF ProtoMat circuit plotter. The PDMS ($\epsilon_r = 2.7$, $\tan\delta = 0.0027$) was spun on the antenna in liquid form and then cured in an oven for hardening. The liquid metal (Alfa Aesar, product no. 12478) has a composition of Ga:In of 75.5:24.5 by weight and has a conductivity $\sigma_{\text{EGaIn}} = 3.46 \times 10^6$ S/m. The return loss of the antenna for each operating state was measured using a vector network analyzer (VNA). Figs. 5 and 7 show the measured return loss of the antenna for the four different states. The plot

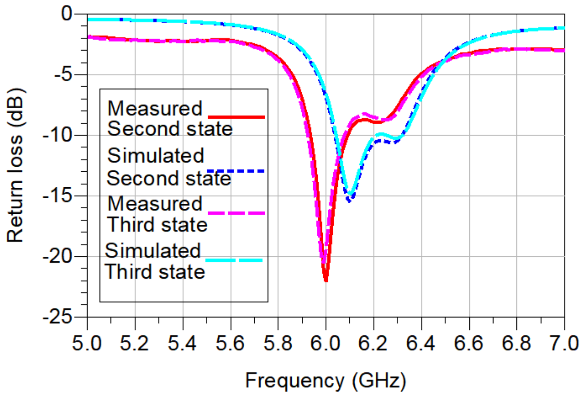

Fig. 7. Measured return loss second and third states CP.

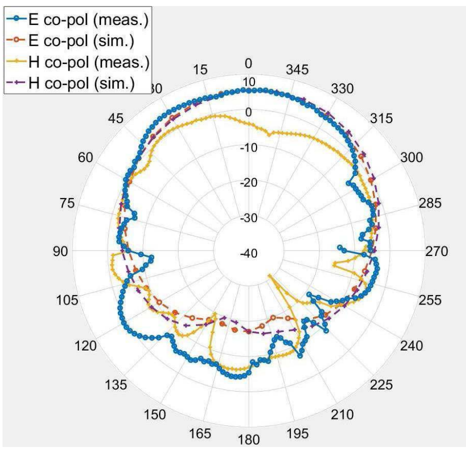

(a)

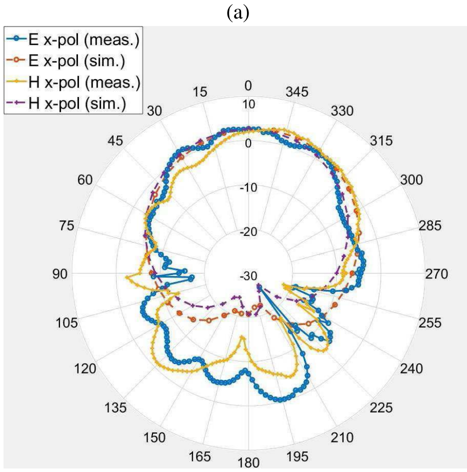

(b)

Fig. 8. Measured (a) co-pol and (b) x-pol radiation patterns in decibel for the second state (LHCP) at 6 GHz.

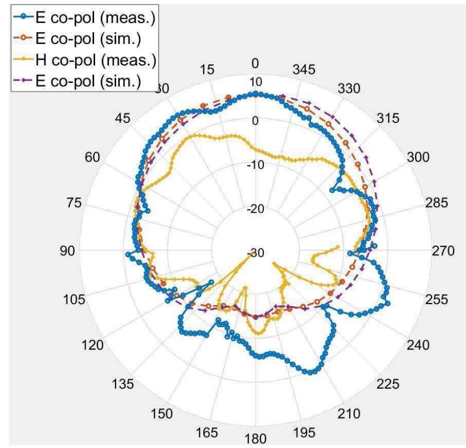

(a)

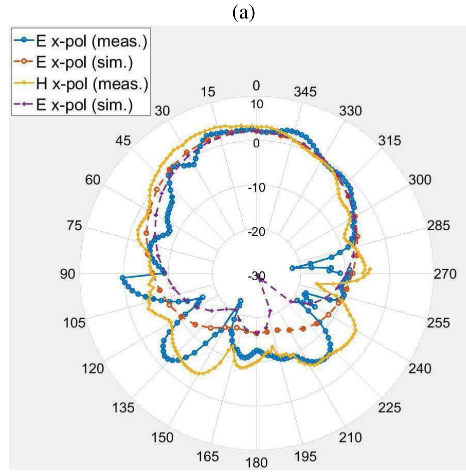

(b)

Fig. 9. Measured (a) co-pol and (b) x-pol radiation patterns in decibel for the third state (RHCP) at 6 GHz.

shows that the antenna's frequency is tuned over the range 5.8–6.2 GHz and the minimum return loss is better than −16 dB for all cases.

Radiation patterns were measured using an anechoic chamber at Queen's University for each antenna state at the frequency where the lowest return loss was observed for that state with the VNA. In all cases, the axial ratios (ARs) were measured from 5 to 7 GHz with steps of 0.02 GHz and a plot of the result is shown in Fig. 4. The AR was determined using the rotating-source method where the source antenna is linearly polarized and it is rotated to measure the difference between the received power of the two main orthogonal components [18]. Radiation efficiency was calculated using the maximum gain and the directivity by measuring the half-power beamwidths of the E- and H-planes. It is well known that the circular patch antennas have a high efficiency, around 90%.

A. First State: First Operating Frequency and Linear Polarization

The measured co-pol and cross-pol radiation patterns are shown in Fig. 6(a) and (b), respectively. The measured and simulated return losses of the antenna operating under LP mode are shown in Fig. 5. The return loss is better than −16 dB, the efficiency is 88%, and the high AR value shown in Fig. 4 demonstrates the LP of the radiated waves. There is a good agreement between measured and simulated results. Backside radiation in the measured results and the H co-pol asymmetry might be explained because the fabrication process introduces some changes in the antenna's dimensions, the losses of the connector and the putty containers, and the asymmetrical location of the C slot along the H-plane axis.

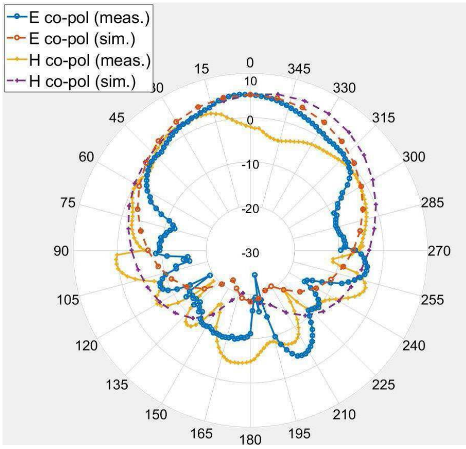

(a)

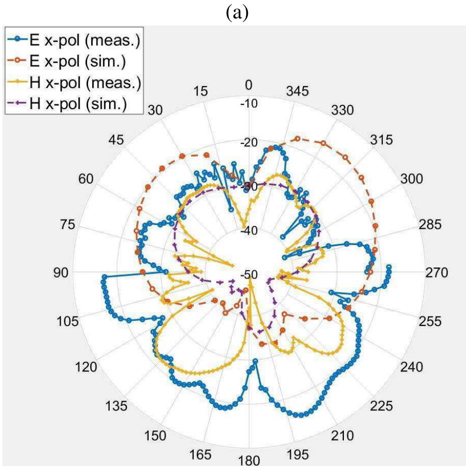

(b)

Fig. 10. Measured (a) co-pol and (b) x-pol radiation patterns in decibel for the third state (LP) at 6.15 GHz.

This is the worst case of the efficiency that is around 1%–2% lower than the other cases.

B. Second and Third States: Second Operating Frequency and LH or RH Circular Polarization

The radiation patterns are similar to the first state radiation pattern. The measured left-hand circular polarization (LHCP) co-pol and cross-pol radiation patterns are shown in Fig. 8(a) and (b), respectively. The AR is less than 3 dB from 5.84 to 6.27 GHz and the return loss is better than −16 dB as shown in Fig. 7 and the efficiency is 90.6%. The measured right-hand circular polarization (RHCP) co-pol and cross-pol radiation patterns are shown in Fig. 9(a) and (b). The AR is less than 3 dB from 5.82 to 6.1 GHz. Fig. 7 shows the return losses of the antenna operating under RHCP. The return losses are better than −10 dB and the efficiency is 90%. In both cases, the AR shown in Fig. 4 demonstrates the CP of the radiated waves. Some additional sources of disagreement between the measured and simulated results, besides those noted earlier, are the differences in the thickness, positions, and shapes of the liquid metal rectangles. Note that the liquid metal has a stronger effect on the H co-pol pattern which looks less symmetrical, especially in the case of RHCP. This effect can be attributed to the thickness of the liquid metal rectangles which can be around 5–10 times thicker than simulated.

C. Fourth State: Third Operating Frequency and Linear Polarization

The radiation patterns are similar to the first state radiation patterns and these are shown in Fig. 10(a) and (b). The return loss of the antenna is shown in Fig. 5 and it is better than −10 dB and the efficiency is 89%. In this case, the H co-pol has the same asymmetry in the right side discussed in the previous sections. Backside radiation levels in the measured results might be explained because the existence of undesirable reflections in the ground plane of the antenna.

There is an unexpected effect of impedance matching that might be attributed to the combined effects of the liquid metal and the putty containers, which generates an improvement in the return loss being even better than the simulated case using a perfect conductor liquid metal switch [9].

IV. Conclusion

An antenna with linear and CPs using two putty containers and liquid metal was designed and simulated. The results show the viability of using liquid metal in a simple way to get frequency and polarization reconfigurability by changing the position of the liquid metal on the top of a circular patch antenna with a C-shaped slot. The antenna can be operated under the LP in all the states. Moreover, it can be operated under LH or RH CP at 6 GHz. Mechanical–electrical systems are required to control the RF switches and they will negatively affect the performance of the antenna. A linear behavior is the main advantage of using liquid metal to generate a short circuit on the surface of the circular patch antenna instead of diodes. The effects of the liquid metal on the efficiency are negligible (lower than 3%) because the small area of the liquid metal drops compared to the total antenna area. In addition, undesired effects such as radiation efficiency degradation, decreasing of the gain, and decreasing of the power handling due to the p-i-n diodes insertion loss or isolation can be reduced by using liquid metal.

References

[1] M. Borhani, P. Rezaei, and A. Valizade, "Design of a reconfigurable miniaturized microstrip antenna for switchable multiband systems," *IEEE Antennas Wireless Propag. Lett.*, vol. 15, pp. 822–825, 2016.

[2] S.-J. Wu and T.-G. Ma, "A wideband slotted bow-tie antenna with reconfigurable CPW-to-slotline transition for pattern diversity," *IEEE Trans. Antennas Propag.*, vol. 56, no. 2, pp. 327–334, Feb. 2008.

[3] M. A. Hossain, I. Bahceci, and B. A. Cetiner, "Parasitic layer based radiation pattern reconfigurable antenna for 5G communications," *IEEE Trans. Antennas Propag.*, vol. 65, no. 12, pp. 6444–6452, Dec. 2017.

[4] P. Zhang, Y. Cui, and R. Li, "A novel polarization reconfigurable circularly polarized antenna," in *Proc. IEEE AP-S Symp.*, Jul. 2017, pp. 2215–2216.

[5] A. Petosa, *Frequency-Agile Antennas for Wireless Communications*. Norwood, MA, USA: Artech House, 2013.

[6] D. Guha and Y. M. M. Antar, Eds., *Microstrip and Printed Antennas: New Trends, Techniques and Applications*. Hoboken, NJ, USA: Wiley, 2011.

[7] M. Shirazi, T. Li, and X. Gong, "Effects of PIN diode switches on the performance of reconfigurable slot-ring antenna," in *Proc. IEEE 16th Annu. Wireless Microw. Technol. Conf. (WAMICON)*, Apr. 2015, pp. 1–3.

[8] D. Rodrigo, L. Jofre, and B. A. Cetiner, "Circular beam-steering reconfigurable antenna with liquid metal parasitics," *IEEE Trans. Antennas Propag.*, vol. 60, no. 4, pp. 1796–1802, Apr. 2012.

[9] K. Entesari and A. P. Saghati, "Fluidics in microwave components," *IEEE Microw. Mag.*, vol. 17, no. 6, pp. 50–75, Jun. 2016.

[10] A. Arbelaez-Nieto, J.-L. Olvera-Cervantes, C. E. Saavedra, and A. Corona-Chavez, "Balanced liquid metal reconfigurable microstrip filter," *J. Electromagn. Waves Appl.*, vol. 31, no. 14, pp. 1453–1466, 2017.

[11] M. Abdallah and C. E. Saavedra, "Fluidically-tuned reflection oscillator at C-band," in *Proc. Int. Symp. Antenna Technol. Appl. Electromagn. (ANTEM)*, Aug. 2018, pp. 1–3.

[12] A. Pourghorban Saghati, J. Batra, J. Kameoka, and K. Entesari, "A miniaturized microfluidically reconfigurable coplanar waveguide bandpass filter with maximum power handling of 10 watts," *IEEE Trans. Microw. Theory Techn.*, vol. 63, no. 8, pp. 2515–2525, Aug. 2015.

[13] Y. Lu and S.-Y. Chen, "A modified U-slot patch antenna with full polarization agility," in *Proc. IEEE 5th Asia–Pacific Conf. Antennas Propag. (APCAP)*, Jul. 2016, pp. 9–10.

[14] P.-Y. Qin, A. R. Weily, Y. J. Guo, and C.-H. Liang, "Polarization reconfigurable U-slot patch antenna," *IEEE Trans. Antennas Propag.*, vol. 58, no. 10, pp. 3383–3388, Oct. 2010.

[15] M. Fakharian, P. Rezaei, and A. Orouji, "Reconfigurable multiband extended U-slot antenna with switchable polarization for wireless applications," *IEEE Antennas Propag. Mag.*, vol. 57, no. 2, pp. 194–202, Apr. 2015.

[16] P.-Y. Qin, Y. J. Guo, Y. Cai, E. Dutkiewicz, and C.-H. Liang, "A reconfigurable antenna with frequency and polarization agility," *IEEE Antennas Wireless Propag. Lett.*, vol. 10, pp. 1373–1376, Dec. 2011.

[17] I. Wolff and N. Knoppik, "Rectangular and circular microstrip disk capacitors and resonators," *IEEE Trans. Microw. Theory Techn.*, vol. MTT-22, no. 10, pp. 857–864, Oct. 1974.

[18] B. Y. Toh, R. Cahill, and V. F. Fusco, "Understanding and measuring circular polarization," *IEEE Trans. Educ.*, vol. 46, no. 3, pp. 313–318, Aug. 2003.